Wei, Y., Fränz, M., Dubinin, E., Woch, J., Lühr, H., Wan, W., Zong, Q.-G., Zhang, T. L., Pu, Z. Y., Fu, S. Y., Barabash, S., Lundin, R., Dandouras, I. (2012): Enhanced atmospheric oxygen outflow on Earth and Mars driven by a corotating interaction region. - Journal of Geophysical Research, 117, A3

DOI: 10.1029/2011JA017340

Enhanced atmospheric oxygen outflow on Earth and Mars driven by a corotating interaction region

Y. Wei,[1] M. Fraenz,[1] E. Dubinin,[1] J. Woch,[1] H. Lühr,[2] W. Wan,[3] Q.-G. Zong,[4] T. L. Zhang,[5] Z. Y. Pu,[4] S. Y. Fu,[4] S. Barabash,[6] R. Lundin,[6] and I. Dandouras[7,8]

Received 6 November 2011; revised 4 January 2012; accepted 6 January 2012; published 9 March 2012.

[1] Solar wind controls nonthermal escape of planetary atmospheric volatiles, regardless of the strength of planetary magnetic fields. For both Earth with a strong dipole and Mars with weak remnant fields, the oxygen ion (O^+) outflow has been separately found to be enhanced during corotating interaction region (CIR) passage. Here we compared the enhancements of O^+ outflow on Earth and Mars driven by a CIR in January 2008, when Sun, Earth, and Mars were approximately aligned. The CIR propagation was recorded by STEREO, ACE, Cluster, and Mars Express (MEX). During the CIR passage, Cluster observed enhanced flux of upwelling oxygen ions above the Earth's polar region, while MEX detected an increased escape flux of oxygen ions in the Martian magnetosphere. We found that (1) under a solar wind dynamic pressure increase of 2–3 nPa, the rate of increase in Martian O^+ outflow flux was 1 order higher than those on Earth; and (2) as a response to the same part of the CIR body, the rate of increase in Martian O^+ outflow flux was on the same order as for Earth. The comparison results imply that the dipole effectively prevents coupling of solar wind kinetic energy to planetary ions, and the distance to the Sun is also crucially important for planetary volatile loss in our inner solar system.

Citation: Wei, Y., et al. (2012), Enhanced atmospheric oxygen outflow on Earth and Mars driven by a corotating interaction region, *J. Geophys. Res.*, *117*, A03208, doi:10.1029/2011JA017340.

1. Introduction

[2] Earth and Mars probably had similar primitive atmospheres, but evolved in different ways in the following several billion years. The escape of planetary volatiles forced by solar wind is thought to be the most important reason for such a discrepancy, since Earth's strong dipole can effectively shield its atmosphere from direct interaction with solar wind while Mars's weak crustal field cannot [*Lundin et al.*, 2007; *Lammer et al.*, 2008]. Recently, comparison of volatile escape rates on Earth and Mars/Venus led to a new doubt on this conventional wisdom: the larger Earth's magnetosphere intercepts and tunnels down to the ionosphere more energy from the solar wind than more compact interaction regions of nonmagnetized planets, thus the expected shielding of the Earth atmosphere by the intrinsic magnetic field is not as efficient as one may assume [*Barabash*, 2010; *Strangeway et al.*, 2010]. Only an accurate observational estimate of ion escape can solve this controversy. Unfortunately, not until the recent 3 years did we realize that very low energy singly charged oxygen ions (O^+) may constitute a significant part of total O^+ escape flux on Mars [*Lundin et al.*, 2008a; *Fränz et al.*, 2010], as theoretically calculated through momentum transfer (see the new reviews by *Lundin et al.* [2007] and *Dubinin et al.* [2011]). A similar situation was also surprisingly found on Earth for H^+ escape [*Engwall et al.*, 2009]. Such very cold ions are not easy to measure due to spacecraft motion, spacecraft potential and other technical problems. In next-generation missions, when the instrumentation will be significantly improved, we will be able to make more direct comparison of the observations on these planets.

[3] The escaping ions are a part of outflowing ions from a planetary ionosphere, the rest of which return to the planetary ionosphere. The knowledge of ion outflow/escape that we have acquired comes largely from the comparison of individual and statistical estimations from different planets. Some important parameters are difficult to consider in statistical studies, such as solar EUV radiation, which is

[1]Max Planck Institute for Solar System Research, Katlenburg-Lindau, Germany.
[2]German Research Centre for Geosciences, Potsdam, Germany.
[3]Institute of Geology and Geophysics, Chinese Academy of Sciences, Beijing, China.
[4]School of Earth and Space Sciences, Peking University, Beijing, China.
[5]Space Research Institute, Austrian Academy of Sciences, Graz, Austria.
[6]Swedish Institute of Space Physics, Kiruna, Sweden.
[7]L'Observatoire Midi-Pyrénées, Université Paul Sabatier, Toulouse, France.
[8]Also at Research Institute in Astrophysics and Planetology, National Center for Scientific Research, Toulouse, France.

0148-0227/12/2011JA017340

important for Earth's ionospheric scale height and polar wind [*Yau and Andre*, 1997] and Martian O^+ escape [*Lundin et al.*, 2008b]. One solution proposed here is to compare the simultaneous observations of ion outflow on different planets when they are aligned on the same side of the Sun (conjunction event). Such a case is expected to guarantee the same solar EUV level for these planets, and it will also allow us to examine the role of the Sun–planet distance in planetary atmospheric outflow/escape. In the evolutionary view of planetary atmosphere and habitability, that is, on time scales of millions to billions of years, the distance to the Sun becomes very important. Assuming that the solar wind expansion in the inner solar system is approximately a spherical and symmetrical outward-directed flow, the momentum flux (dynamic pressure) attenuates with a factor $1/R^2$; thus the momentum flux at the present Mars orbit is only 43% of that at Earth orbit.

[4] The ion outflow on both Earth and Mars is highly influenced by solar wind structures [e.g., *Moore et al.*, 1999; *Luhmann et al.*, 2007]. The sustained southward interplanetary magnetic field (IMF) frozen in coronal mass ejections (CMEs) usually triggers magnetic storms and substorms in the Earth's magnetosphere, which can convey solar wind electromagnetic energy into the magnetosphere [*Lu et al.*, 1998] and ultimately drive ion escape above the auroral zone and also contribute to various escape processes. However, there are no similar effects on Mars, because the ion escape from Mars is overwhelmingly driven by solar wind kinetic energy through "cool ion outflow," "plasma clouds," and "ion pick up" [*Lammer et al.*, 2008, p. 415]. On the other hand, corotating interaction regions (CIRs) between the high-speed streams (HSSs) and the ambient solar wind are frequently associated with high solar wind dynamic pressure (SWDP) and with fluctuating IMF rather than sustained southward IMF. On Earth, the SWDP has been found to be a very strong driver of outflows, particularly from the cusp region where the solar wind interaction is quite direct [*Pollock et al.*, 1990; *Moore and Horwitz*, 2007; *Echer et al.*, 2008]. On Mars, recent results showed that SWDP was also clearly related to a large increase of ion outflow [*Dubinin et al.*, 2009; *Edberg et al.*, 2010]. Therefore, it is feasible to study the influence of solar wind dynamic pressure on ion outflow at Earth and Mars/Venus with the observations during a CIR event.

[5] The Earth-Mars conjunction occurs every 25 months, and the considered case must have also simultaneous O^+ outflow observation on Earth and Mars. Though such cases are quite rare, we found an event in January 2008 serving our purpose fairly well. In this paper we compare the simultaneous observations of O^+ outflow on Earth and Mars during the CIR passage.

2. Spacecraft Position and Instruments

2.1. Spacecraft Position

[6] Figure 1a shows that the Sun, Earth and Mars were approximately aligned on 6 January 2008. If a CIR first hits Earth, there is very high probability for it to propagate to Mars. STEREO-A (STA) and STEREO-B (STB) stayed around the Earth's orbit, and their separation angles from Earth were about 23.0° and 21.2°, respectively. Venus had a large angle (>90°) with respect to Earth and thus did not experience this event.

[7] Mars Express (MEX) is in a highly eccentric polar orbit around Mars with periapsis and apoapsis of about 275 and 10,000 km, respectively. One complete orbit takes ~6.7 h. Figure 1b shows the trajectory of MEX near Mars in the cylindrical coordinate system. According to the averaged positions of bow shock (BS) [*Vignes et al.*, 2000] and magnetospheric boundary (MB) [*Dubinin et al.*, 2006a], MEX stayed in the magnetosheath and crossed the ionosphere during periapsis.

[8] Cluster also has a highly eccentric polar orbit with a period of about 57 h. The trajectories in Figures 1c and 1d only show the interval when upwelling O^+ appeared on 6 January 2008. The magnetic field lines illustrate the simulated magnetosphere by the T96 model [*Tsyganenko*, 1995] through the OVT software (http://ovt.irfu.se/). During the interval of interest, Cluster moved from ~10 to ~5 R_E and, meanwhile, entered the lobe region after crossing the magnetopause from the magnetosheath region.

2.2. Instruments for Observing Oxygen Ion Outflow

[9] The Analyzer of Space Plasma and Energetic Atoms (ASPERA-3) experiment on board MEX is a combination of in situ and remote diagnostics of atmospheric escape induced by the solar wind. It comprises the Ion Mass Analyzer (IMA), Electron Spectrometer (ELS), Neutral Particle Imager (NPI) and Neutral Particle Detector (NPD) [*Barabash et al.*, 2006]. The Ion Mass Analyzer (IMA) determines the composition, energy, and angular distribution of ions in the energy range ~10 eV/q to 30 keV/q. Mass (m/q) resolution is provided by combination of the electrostatic analyzer with deflection of ions in a cylindrical magnetic field set up by permanent magnets. A new patch uploaded in May 2007 has further improved the IMA performance, extending the energy range down to cold/low-energy ions (≤10 eV). In the energy range ≥50 eV, IMA measures fluxes of different (m/q) ion species with a time resolution of 192 s and a field of view of 90° × 360° (electrostatic sweeping provides an elevation coverage of ±45°). The measurements of the cold/low-energy component (≤50 eV) are carried out without the elevation coverage but with an increased time resolution of these 2-D measurements of 12 s. The ELS sensor measures 2D distributions of the electron fluxes in the energy range 1 eV to 20 keV with a field of view of 4° × 360° and a time resolution of ~4 s. A grid usually biased at ~5 V protects the sensor from the low-energy photoelectrons.

[10] The Cluster Ion Spectrometer (CIS) is a comprehensive ionic plasma spectrometry package on board the Cluster, capable of obtaining full three-dimensional ion distributions with one spin (4 s) time resolution and with m/q composition determination [*Rème et al.*, 2001]. The CIS instrument consists of two sensors, the Composition Distribution Function Analyzer (CODIF) and the Hot Ion Analyzer (HIA). The CODIF measures three-dimensional distribution functions of the major ion species over the energy range 30 eV/q to 40 keV/q. It is a combination of a top hat electrostatic analyzer followed by a post acceleration of 15 kV and then a time of flight (TOF) measurement. It can resolve the major ion species, H^+, He^+, He^{++}, and O^+. The detector has a field of view of 360° orthogonal to the spin plane, divided

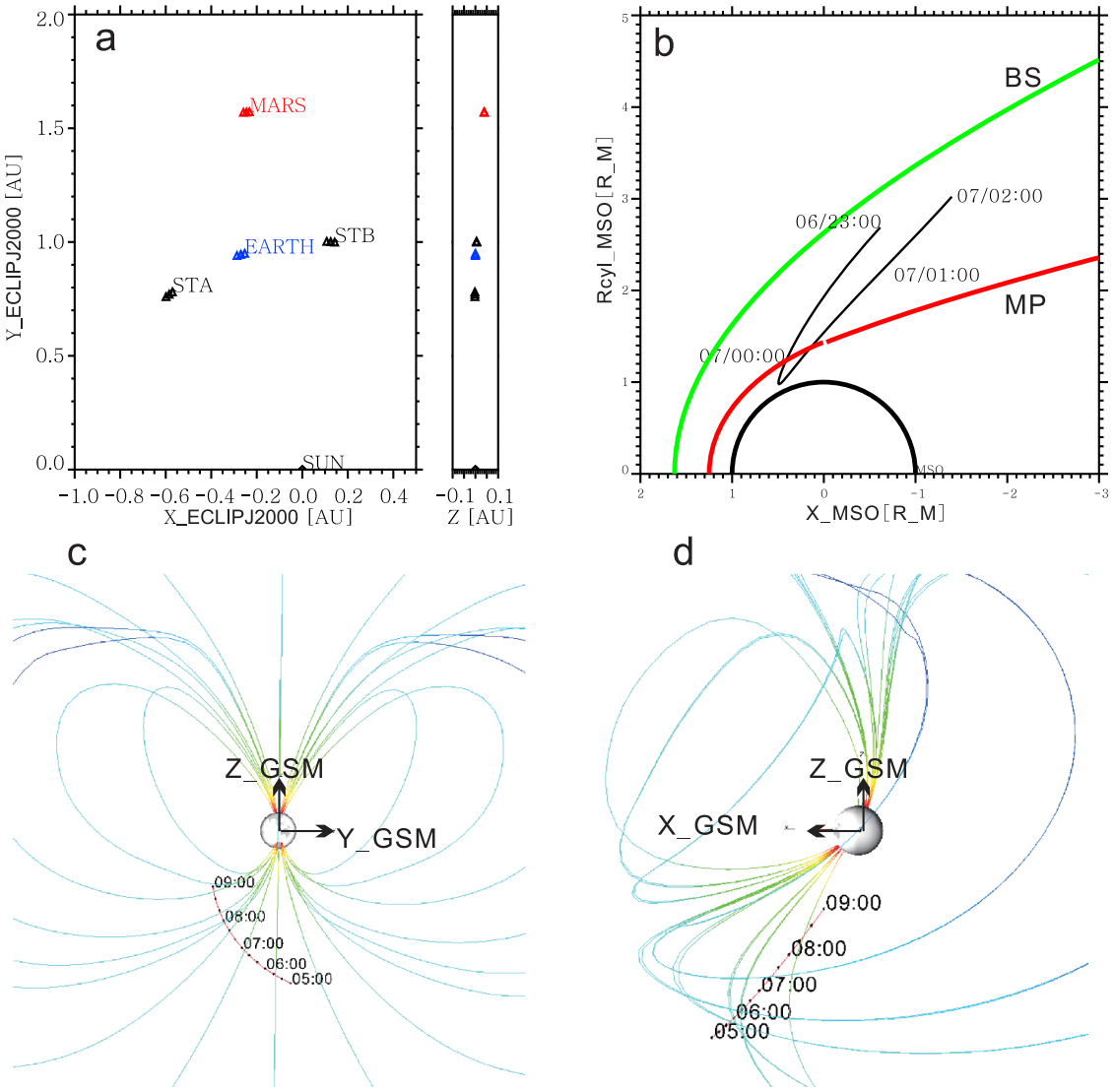

Figure 1. (a) Positions of STEREO, Earth, and Mars on 6 January 2008. (b) Trajectory of Mars Express (MEX) around the periapsis at 00:00 UT, 7 January 2008. The positions of the bow shock (BS) and magnetopause (MP) are taken from model; see the text. (c, d) Trajectory of Cluster on 6 January 2008 on *Y-Z* and *X-Z* planes in GSM coordinates, respectively.

into 16 sectors of 22.5° each. The angular resolution is about 22.5° in the spin plane.

3. Observations

3.1. CIR Propagation and Geoeffectiveness

[11] The CIR successively hit STB, Earth, STA and Mars. Figure 2 shows 1 h resolution data of the STEREO and OMNI database during 2–9 January 2008. For this case, OMNI adopts Wind data before 03:00 UT, 5 January and ACE data after this moment, respectively, and then shifts them to 1 AU. The CIR was identified by compressed total magnetic field (B_T), increased velocity (V), and proton number density (N). Another feature is the fluctuating magnetic field components, as shown in Figure 3b. To specify the CIR propagation, we use the jump in B_T as an indictor of the CIR due to lack of a clear shock signature, which approximately coincides with the jump in voltage. The arrival times at STB, Earth, and STA were 08:00 UT on 3 January, 23:00 UT on 4 January, and 15:00 UT on 6 January, respectively. Thus the time delays were 39 h from STB to Earth and 40 h from Earth to STA. Considering the 1.8° difference of separation angles, the angular propagation speed of the separation line between high- and low-speed solar wind agrees well with the solar rotation speed of 13.8°/d. However, the proton density evolved to the double-peak shape at Earth and STA.

[12] MEX has no instrument for magnetic field measurement. We can only infer solar wind conditions from the plasma measurements inside the magnetosheath (see Figure 1b). Figure 2 (bottom) shows proton velocity and density, and it shows a jump in V starting from 23:00 UT on 6 January, i.e., 8 h after impacting STA. Note that the periodic drops of the velocity were due to ionospheric crossings.

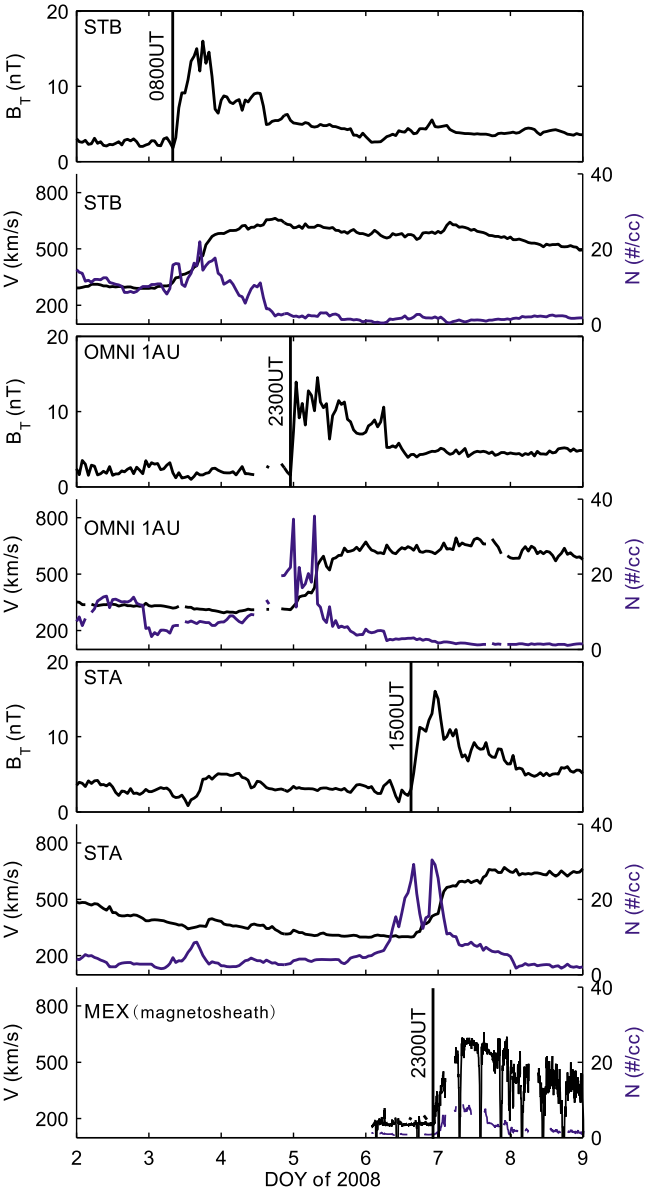

Figure 2. Propagation of the corotating interaction region (CIR) successively recorded by STB, Wind/ACE, STA, and MEX. Three parameters, total magnetic field (B_T), solar wind speed (V), and proton density (N), are shown for each satellite during 2–9 January 2008. The Wind data are adopted before 03:00 UT, 5 January, and ACE data are adopted after this time. Note that MEX does not have magnetic field measurements and is located in the magnetosheath rather than in the solar wind for this case.

After 23:00 UT, the ELS on board MEX in the solar wind recorded a strong electron energization visible from the energy spectrum, where the electron flux increased by 1 order of magnitude (this will be shown in Figure 6). This enhancement persisted over 2 days with gradual attenuation.

[13] The details of the CIR and its geoeffectiveness are shown in Figure 3. The SWDP at Earth orbit fluctuated between 3 and 14 nPa, compared to the 1–2 nPa during the pre-CIR interval. Assuming a spherical expansion of the solar wind, the SWDP at Mars orbit may be inferred from OMNI data by multiplying it by $1/R^2$, where R is 1.52 AU. The symmetric ring current index (*SYMH*) is essentially a high-resolution version of the storm time disturbance index (*Dst*), an indicator of the ring current intensity, which is also sensitive to a rise of SWDP. The *SYMH* shows a sharp jump at 22:45 UT on 4 January, coinciding with the jump in SWDP. The *Kp* index stands for disturbances of the geomagnetic field caused by solar particle radiation within the 3 h interval concerned. Enhancement of the *Kp* index could be the effect of either rise of convectional electric field or rise of auroral conductance, which is usually caused by magnetospheric energetic particle precipitation. The pulses in *SYMH* and *Kp* indices on 5 January were clearly correlated with southward (negative) B_Z, suggesting that they were caused by the entry of solar wind electromagnetic energy into the magnetosphere-ionosphere system through magnetic reconnection on the dayside magnetopause [e.g., *Lu et al.*, 1998]. Unlike CME events, the fluctuating IMF in this CIR does not cause a deposit of much solar wind

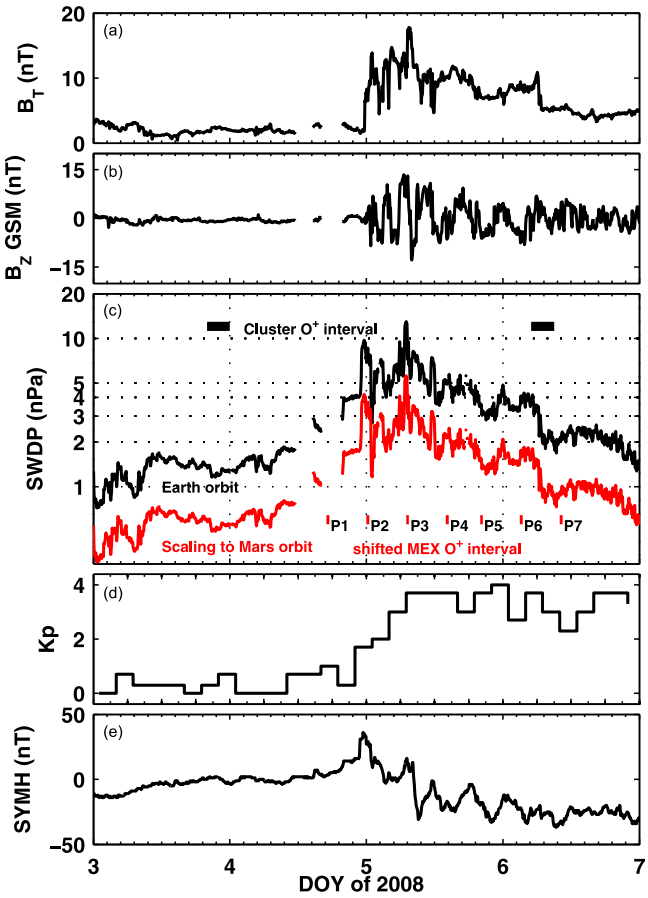

Figure 3. Solar wind conditions at Earth and geomagnetic indices during 3–7 January 2008. (a, b) Total IMF (B_T) and Z component (B_Z). (c) Solar wind dynamic pressure (SWDP) at Earth and also the estimated value at Mars. (d, e) *Kp* index and symmetric ring current *H* index (*SYMH*). The intervals of O^+ observations illustrated here will be shown in Figures 4–8. "P" denotes the periapsis interval in the MEX observation.

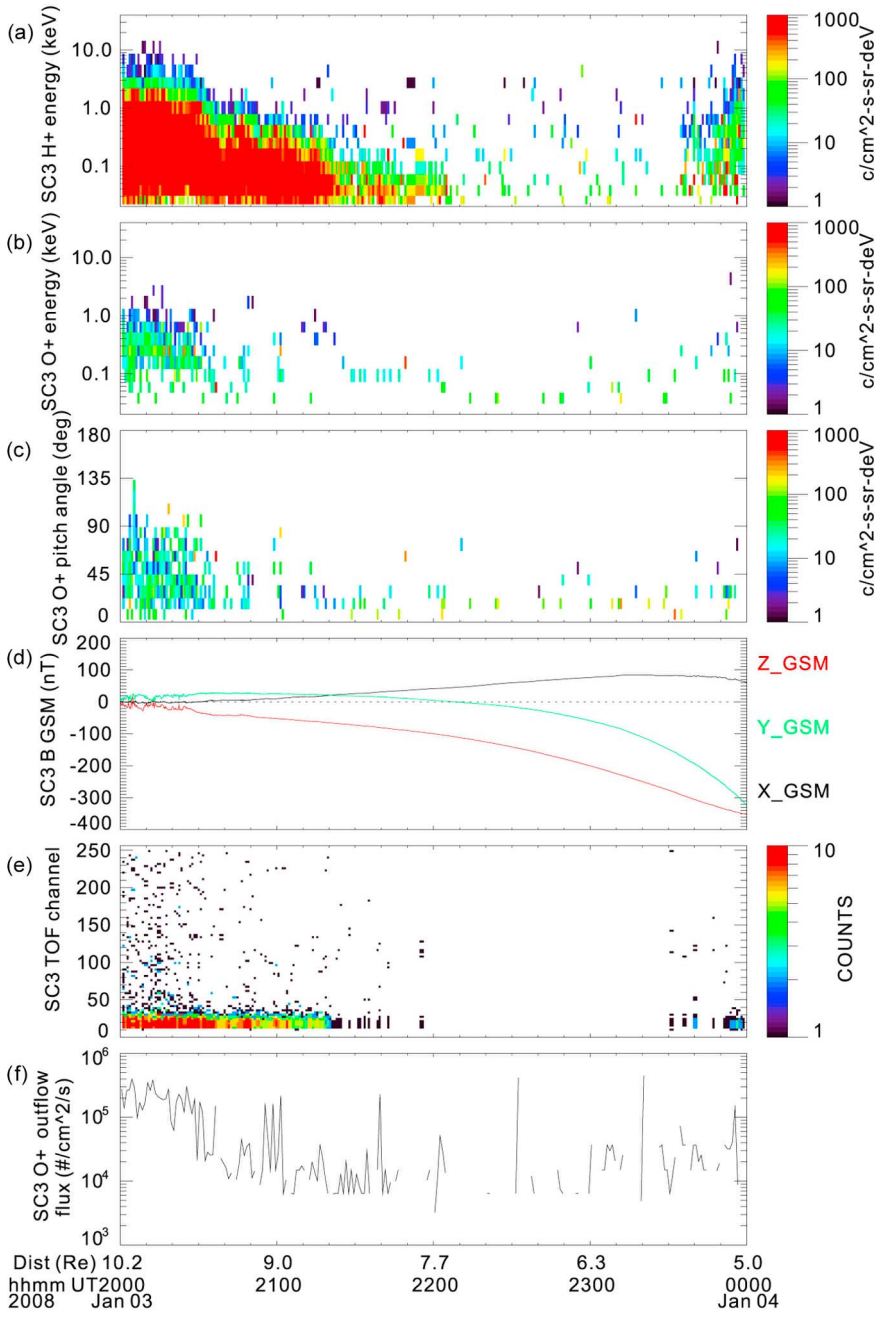

Figure 4. Cluster SC3 (Samba) CODIF observations in the lobe region during quiet time 20:00–24:00 UT on 3 January 2008. (a–c) Time-energy spectrogram of H^+, time-energy spectrogram of O^+, and time-pitch angle distributions. The observed O^+ was outflowing along the field line. (d) Magnetic field line. (e) Counts in the time of flight channels. (f) O^+ outflow flux in all energy ranges (0–40 keV).

electromagnetic energy into the magnetosphere-ionosphere system, according to the moderate *Kp* (≤4) and *SYMH* (≥40 nT) values.

3.2. O^+ Outflow on Earth

[14] In this section we compare the upwelling O^+ observations before and during the CIR, as shown in Figure 4 and Figure 5, respectively. The two intervals have 57 h (1 orbit period) time difference, thus Figures 1c and 1d can provide trajectory information for both intervals. The SWDP values corresponding to the two intervals are marked in Figure 3 by the black bars. During 20:00–24:00 UT on 3 January when the geomagnetic disturbance was very weak, Cluster successively went through the magnetosheath and the southern lobe region. The CODIF H^+ data in Figure 4 show a heated spectrum before 20:30 UT, which is a typical magnetosheath feature. The gradual reductions of H^+ flux and energy during 20:30–22:00 UT were indicative of the cusp region. During 22:00–23:30 UT, Cluster stayed in the lobe region where the magnetic field was relatively strong.

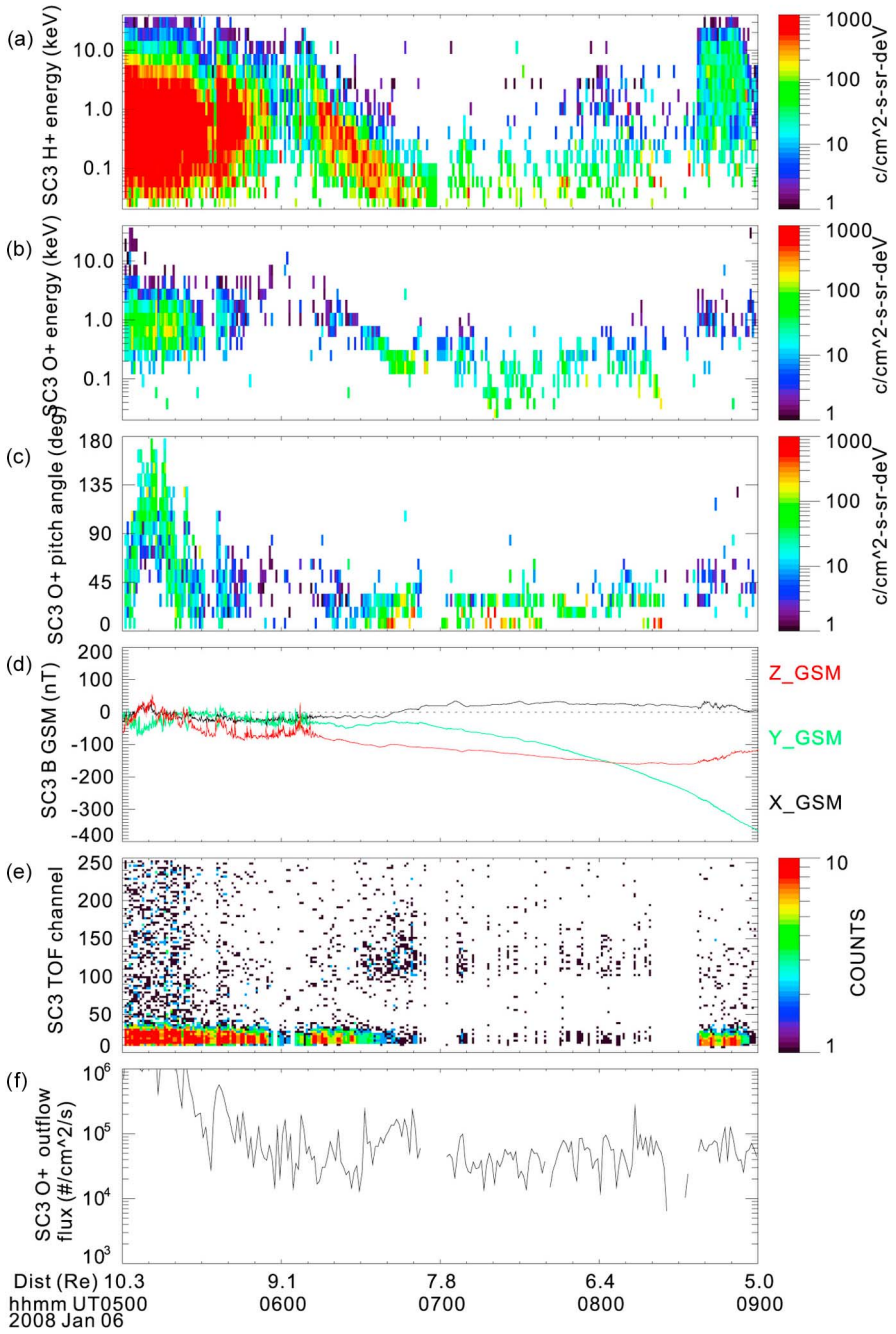

Figure 5. Same as Figure 4 but for 05:00–09:00 UT on 6 January 2008, when the CIR was passing the Earth. Note that Cluster's trajectory during this interval is very close to the interval shown in Figure 4. The O^+ outflow was significantly enhanced, and the magnetic field was compressed by the increased dynamic pressure.

[15] The CODIF uses a TOF technique to distinguish between ion species. When count rates are very high, a fraction of the H^+ counts can spill into the heavy ion TOF ranges because of false coincidences. Such contamination is especially significant in the magnetosheath but generally not remarkable in the lobe. The reliable O^+ signals can be directly discerned from the TOF spectrum. According to the instrument performance [*Rème et al.*, 2001], the O^+ with energy less than 15 keV should peak in the 100–200 TOF channel range. The Figure 4e shows that the protons peaking in the 10–30 TOF channel range, and spilled into all channels before 20:30 UT when the CODIF recorded a few fake O^+ (Figure 4b). The most discernable O^+ counts appeared at 21:55 UT and 23:30–23:50 UT with some counts in 100–150 TOF channel range, and their energy was not higher than 0.1 keV. The pitch angle distribution shows the O^+ ions moved along the field lines; that is, they were subject to ionospheric outflow. The O^+ outflow flux was intermittent,

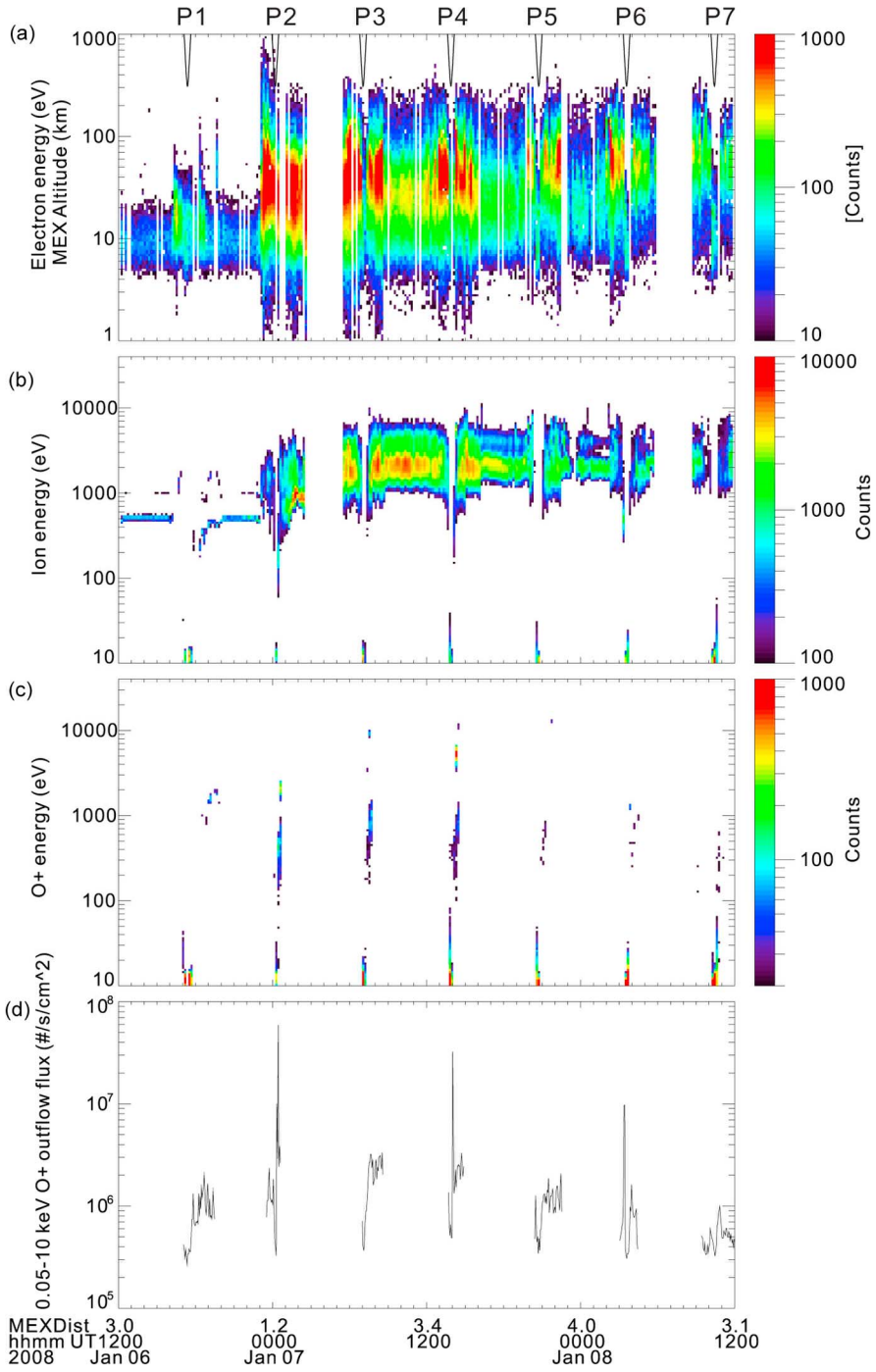

Figure 6. Seven orbit observations by IMA on board MEX from 12:00 UT, 6 January, to 12:00 UT, 8 Janurary 2008. (a) Electron spectrogram with altitude of MEX. The P1–P7 denote seven periapsis passes, which also correspond to those in Figure 3. The interval P1 was under quiet solar wind (pre-CIR). (b, c) All ion energy spectra and O^+ energy spectra observed by IMA. (d) O^+ outflow flux in the energy range 0.05–10 keV.

and seemingly fluctuated around 1×10^4 to 3×10^4 #/cm^2/s. Note that the higher flux during the magnetosheath interval was caused by protons rather than real O^+.

[16] Figure 5 shows overall similar observations but with significant O^+ outflow enhancement. The SWDP during the pre-CIR interval was 1.1 nPa, while during the CIR interval there was a gradual transition from 4 to 2 nPa. The increase of total magnetic field suggested that the magnetosphere was indeed compressed by the high SWDP. Cluster moved into the cusp around 05:30 UT, but returned to the magnetosheath at 05:35 UT, and then entered the cusp again at 06:10 UT when the H^+ flux and energy decreased. The

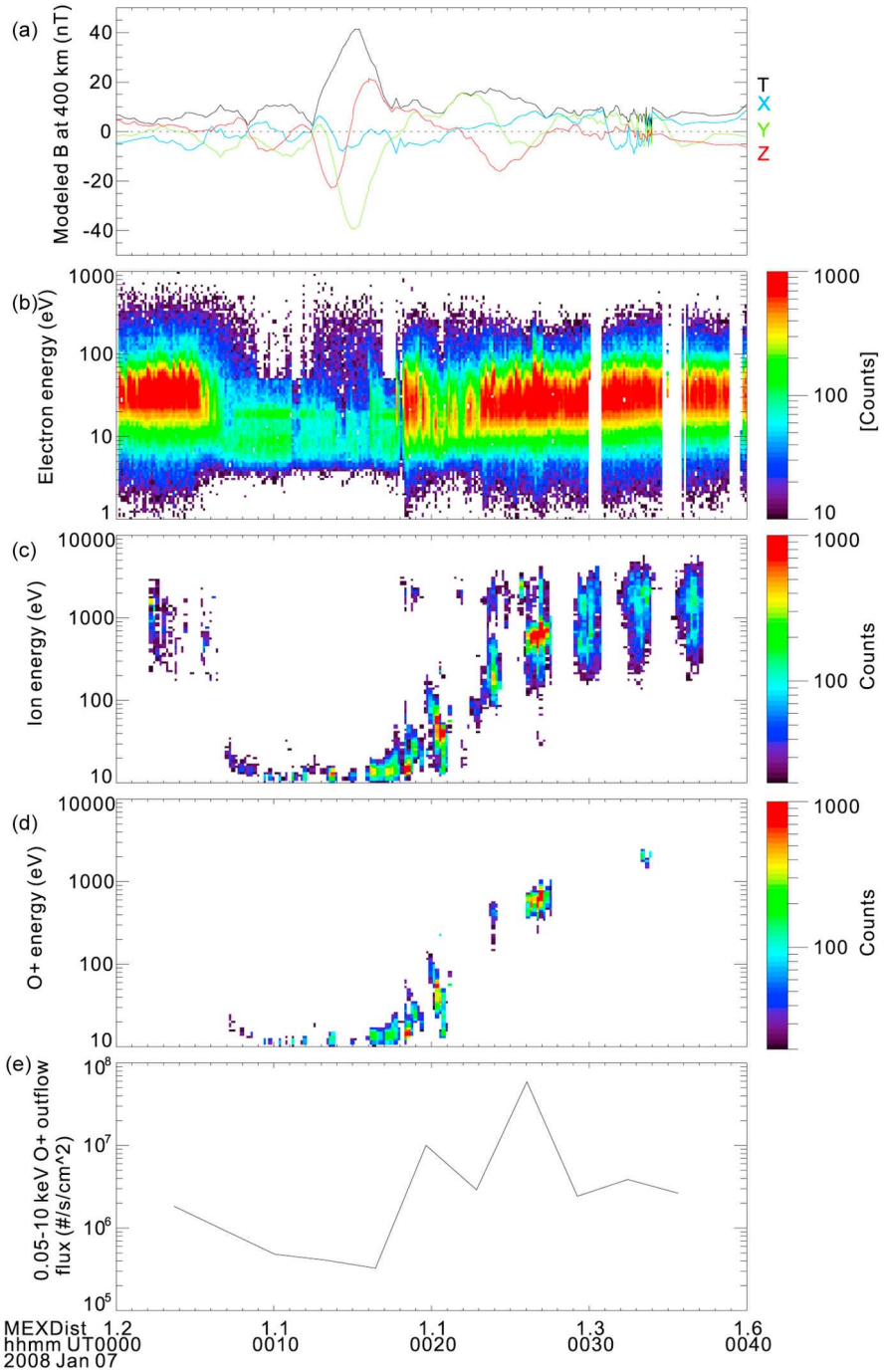

Figure 7. (a) Modeled magnetic field at 400 km. (b–e) Same as in Figure 6, but only for the P2 interval.

motion of the magnetopause was probably triggered by the SWDP variations. There was a narrow beam in the O^+ energy spectrum, of which the energy was less than 1 keV. Such a kind of O^+ outflow in this region has been investigated by several authors using Cluster data, and is usually explained as upwelling O^+ originating from the cusp or dayside auroral region, i.e., the "cleft ion fountain" [e.g., *Nilsson et al.*, 2004, p. 2505; *Arvelius et al.*, 2005; *Zhang et al.*, 2011]. The O^+ outflow flux fluctuated between 2×10^4 to 2×10^5 #/cm^2/s, and the average value was about 4×10^4 #/cm^2/s. The maximum appeared on 06:40–06:50 UT when in the 100–150 TOF channel range an enhancement of counts was recorded. The gap during 06:55–07:00 UT was caused by missing data.

3.3. O^+ Outflow on Mars

[17] Figure 6 shows the continuous observations of electrons and ions by the IMA for about 7 orbits, of which the

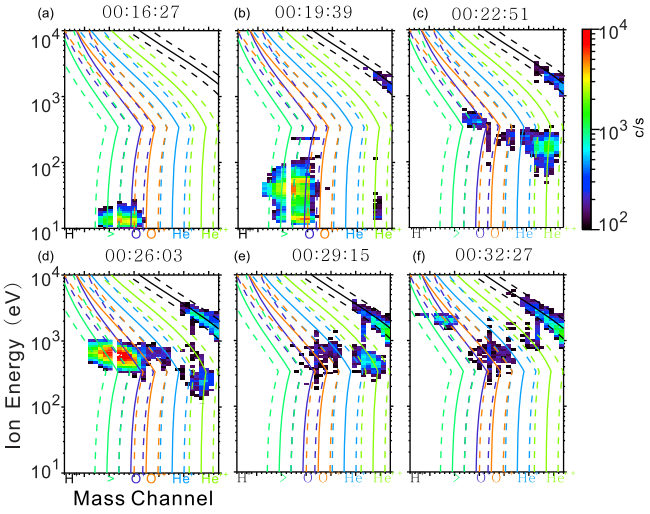

Figure 8. The energy-mass matrix during 00:16–00:33 UT, 7 January 2008 (P2 interval). Vertical axes are energy/charge (E/q), the horizontal axes are the position of the ion impact on the detector (a sensor mass ring, R_m), and the color codes are the counts that were accumulated over all directions and averaged over occurrences. The bold lines represent constant mass, and the corresponding species are marked on each horizontal axis.

first one was during the pre-CIR interval. In Figure 6a, we plot the altitude of MEX near the periapsis to denote the crossings of the solar wind interaction region. These intervals have been also labeled in Figure 3 with 48 h time shift. From the electron and ion spectrum depicted in Figures 6a and 6b, respectively, it is easy to identify the CIR effects by the expanded energy range and enhanced flux after the shock crossing at 23:00 UT on 6 January.

[18] Now we describe the detailed observations of ion outflow in the interaction region between solar wind and Martian ionosphere. Figure 7 shows the observations around the first periapsis during the CIR passage. The MEX entered the induced magnetosphere at 00:06 UT when the magnetosheath electron flux dropped. During 00:07–00:16 UT, there was a narrow peak in the range between 20 and 30 eV on the electron energy spectra. These ionospheric photoelectrons are produced in association with absorption of the strong HeII line at 30.4 nm in the carbon dioxide dominated atmosphere on Mars [e.g., *Frahm et al.*, 2006]. The ionospheric ions are mainly observed with energy less than 20 eV. They are low-energy O^+ and O_2^+, as seen from the energy-mass matrix in Figure 8. Note that the energy-mass matrixes shown here with a time resolution of 192 s cover the whole field of view of 90° × 360°.

[19] The magnetopause on the outbound leg of the orbit was ambiguous. The MEX reached 398 km above the Martian surface at 00:18 UT, meanwhile, the magnetosheath electron flux abruptly appeared, and there were also significant ion counts concentrated around 2 keV. These magnetosheath ions are usually used to identify the magnetopause [e.g., *Dubinin et al.*, 2006a], however, for our event, the typical 0.2–5 keV sheath protons appeared after 00:30 UT. On the other hand, during 00:18–00:30 UT, the ionospheric O^+ were accelerated from 20 eV to 1 keV in this region and then reached 2 keV in the magnetosheath. As shown in Figure 8b (00:19:39 UT), the ionospheric O^+ and magnetosheath H^+ coexisted during this interval. Thus, the MEX went through a thick interaction region where solar wind plasma protruded into the induced magnetosphere and energized ionospheric ions to leave Mars, as discovered by earlier IMA observations [*Lundin et al.*, 2004; *Dubinin et al.*, 2006b]. The crustal field from the model by *Cain et al.* [2003] in this region was not strong, less than 20 nT (Figure 7a), and this could be a preferable condition for solar wind plasma protrusion [*Fränz et al.*, 2006]. The coexistence of solar wind ions and accelerated Martian ions suggest that the Martian ions acquired momentum through direct interaction with the shocked solar wind. Such kind of O^+ acceleration has been interpreted by two different mechanisms. One is transfer of solar wind momentum to the ionospheric ions [*Pérez-de-Tejada*, 1998], probably through wave-particle interaction [*Dobe et al.*, 1999; *Pérez-de-Tejada et al.*, 2010]. For this mechanism the Martian ions should mainly outflow from the two magnetic polar regions [*Pérez-de-Tejada et al.*, 2009]. The other mechanism, as shown by the statistical results on Mars [*Dubinin et al.*, 2006c] and Venus [*McEnulty et al.*, 2010], is that these ionospheric ions are picked up due to an effective penetration of the solar wind electric field deep into the ionosphere or generation of large fields within the ionosphere. For this mechanism the Martian ions mainly outflow from the positive electric field hemisphere. The importance of both mechanisms may be comparable, but further discussion is beyond the goal of this paper.

[20] Figures 7 and 8 show that there were a lot of O^+ ions below 50 eV, however, we do not count this part into the outflow flux. The first reason is that IMA measures the cold/low-energy component (≤50 eV) without the elevation coverage in order to acquire a higher time resolution of 12 s. The 2-D measurement may seriously underestimate the tailward flow when the velocity of a coming particle has a larger angle with respect to the field of view plane. The second reason is that the velocity of heavy ions with this energy cannot be accurately measured due to the effect of the spacecraft potential, and probably the spacecraft's motion [e.g., *Fränz et al.*, 2010]. These effects exist for the full energy range, but it is less significant for the higher energy band. Therefore, we only calculate the 0.05–10 keV O^+ outflow flux. The O^+ flux in Figure 7e shows two peaks. The peak near 00:20 UT was contributed by 0.05–0.2 keV O^+, while the other peak near 00:26 UT was created by 0.5–1 keV O^+. In the magnetosheath, the O^+ flux largely dropped (~00:33 UT). Note that the very cold O^+ flux during 00:10–00:18 UT could be significant [*Fränz et al.*, 2010], but it is not considered here.

[21] Now let us return to Figure 6. Near each periapsis, there were 2–20 keV pick up O^+ ions in the magnetosheath and <50 eV cold O^+ ions inside the ionosphere (Figure 6d). However, the spikes in the outflow flux mainly came from 0.05–2 keV O^+. The three spikes during P2, P4 and P6 are 6×10^7, 3×10^7, and 1×10^7 #/cm^2/s, respectively, which are above 1 order of magnitude higher than the pre-CIR level of 1×10^6 #/cm^2/s. There are no spikes during P3, P5 and P7, probably caused by a change of interplanetary electric field orientation, which determines the

moving direction of pick up ions [*Luhmann et al.*, 2007]. The high fluxes in the magnetosheath intervals (e.g., 01:00–03:00 UT, 7 January) were produced by the spill-over solar wind protons rather than real O^+.

4. Discussion

[22] We have analyzed the Cluster and MEX observations before and during a CIR passage. The O^+ outflow observed above Earth's polar region was consistent with a cusp origin scenario [e.g., *Nilsson et al.*, 2004; *Kistler et al.*, 2010a; *Zhang et al.*, 2011]. The statistical studies revealed that the outflow rate from the cusp is sensitive to solar wind kinetic energy [*Moore and Horwitz*, 2007] but not related to geomagnetic activity level [*Yau and Andre*, 1997]. The O^+ outflow observed around the Martian magnetopause was probably produced by the pick up process or other momentum transfer mechanisms [*Dubinin et al.*, 2011; *Pérez-de-Tejada*, 1998]. All these mechanisms prefer solar wind kinetic energy, thus such kind of O^+ outflow depends on solar wind momentum flux (SWDP). Therefore, this event allows us to compare the influence of solar wind kinetic energy on O^+ escape at Earth and Mars.

[23] The main purpose of this paper is to examine the ability of the intrinsic magnetosphere at Earth and induced magnetosphere at Mars to prevent solar wind kinetic energy from driving ion escape. The previous comparative studies [e.g., *Barabash*, 2010] on the role of intrinsic magnetosphere, of which the outflow rate were separately derived from observations at different planets, consider the ion outflow that is driven by various solar EUV level and solar wind transits (CME and CIR). Our conjunction event can guarantee the same solar wind transits as drivers for both planets, though we have no large data coverage. The most important information extracted from a case study may be the maximum of the O^+ outflow at the same place driven by the same energy sources. A maximum stands for an extreme status that the ion outflow can be driven to. In other words, an upper limit that O^+ outflow rate can reach tells us how effective the protecting effect of the magnetosphere is.

[24] The P2 interval of MEX observations showed the very early responses after the CIR impacted on Mars, while Cluster only captured the responses 30 h later. However, since the corresponding SWDP at Mars and Earth were decreasing from 4 to 3 nPa and 4 to 2 nPa (Figure 3), respectively, these two intervals can be used to identify the difference of O^+ outflow enhancements on Earth and Mars under similar SWDP. Taking the observation around 06:40 UT in Figure 5, for example, a 200 eV O^+ ion takes ~15 min to travel ~7 R_E along a field line to reach Cluster, therefore this time delay is negligible when we examine the O^+ flux for several hours. The observations during the CIR have shown that the flux maximum increased by ~7 times from 3×10^4 to 2×10^5 #/cm^2/s on Earth when the SWDP increased from ~1.2 to 2–4 nPa, while it increased 60 times from 1×10^6 to 6×10^7 #/cm^2/s on Mars (P2 interval) when the SWDP increased from ~1 to 3–4 nPa. Obviously, the Martian O^+ outflow flux is more sensitive to a SWDP increment. Another comparison considered here is the responses on Earth and Mars to the same part of CIR body. In our event, the MEX P6 interval was very close to the Cluster interval (Figure 3), and it was shown that the O^+ outflow flux increased by 10 times from 1×10^6–1×10^7 #/cm^2/s. The value 10 times on Mars is indeed of the same order as the value 7 times on Earth. This implicates that the attenuated SWDP can still cause a rate of increase in Martian O^+ outflow flux in the same or higher level of those on Earth.

[25] There are two important caveats regarding the estimates of O^+ outflow fluxes. First, the global O^+ outflow processes are dynamic and have spatial and temporal dependences. The observations by the XMM-Newton Earth orbiter telescope independently suggested that the plasma distribution in Martian wake was asymmetric [*Dennerl et al.*, 2006], and *Pérez-de-Tejada et al.* [2009] argued that these observations are consistent with the picture that the transport of solar wind momentum to the Mars ionosphere is more effective over the magnetic polar region. Since the magnetic polar region is dependent on the IMF orientation and the IMF fluctuates inside the CIR, the absence of flux spikes during P3, P5 and P7 can also be understood as that the MEX trajectory is far from the polar region. Because a single spacecraft can only measure O^+ flux along its trajectory, thus it always misses some important information, no matter whether performing case studies or statistical work. This may be an important reason for the large discrepancy in the outflow rates at Mars ever published by different authors, as summed up by *Dubinin et al.* [2011]. Taking Mars, for example, *Barabash et al.* [2007] estimated a maximum of the O^+ outflow flux in the magnetosheath at 1×10^6 #/cm^2/s [see *Barabash et al.*, 2007, Figure 2, left], which corresponds to the pre-CIR level (P1) in our case. As for Earth, the observed O^+ flux could vary with location [*Arvelius et al.*, 2005]. However, this kind of uncertainty caused by spatial dependence may be relatively smaller in case study, because we only compare the measurements by the same instruments at the same place. Second, different calculation methods of O^+ flux, according to different considerations, result in different estimations. Our case was also listed in the statistical work by *Edberg et al.* [2010], but their conclusion is that "the ion fluxes are observed to increase by a factor of ~2.5, on average" [*Edberg et al.*, 2010, p. 4], though they also only considered the O^+ ions with energy larger than 50 eV, as we did. On the other hand, *Dubinin et al.* [2009] showed that during a CIR the O^+ outflow rate was estimated to increase by a factor of ~10. This factor is similar to the P6 interval in our case, which shows the O^+ flux 1×10^7 #/cm^2/s comparing to the pre-CIR level 1×10^6 #/cm^2/s. In addition, based on Pioneer Venus Orbiter (PVO) observations, *Luhmann et al.* [2007] suggested that the total ion flux could increase by a factor of 100 during CMEs.

[26] We have discussed the effect of solar wind kinetic energy on the O^+ escape at Earth and Mars. However, the global O^+ outflow at Earth has another two source regions, polar cap and auroral oval, from which the outflow rates are related to geomagnetic activity [*Yau and Andre*, 1997]. For completeness, it is worth to discuss the total O^+ outflow rate. Previous statistical studies suggested that the total O^+ outflow rate is positively proportional to $\exp(0.5Kp)$ under the same solar EUV level [*Yau et al.*, 1988]. For the two intervals when Cluster observed O^+, the total O^+ outflow rate

increases by 3–7 times when *Kp* increases from 0–1 to 3–4. Since the O^+ outflow rate from cusp/cleft is comparable to that from polar cap and auroral oval during quiet condition (*Kp* = 0–2) [*Yau and Andre*, 1997], the cusp source is expected to become more important when it is observed to increase by 7 times. Overall, for our event, the total O^+ outflow rate would increase by less than 1 order.

[27] The percentage of escape rate to outflow rate at Earth has been rarely studied due to lack of enough measurements. *Seki et al.* [2001] had summarized the total O^+ loss rate from the dayside magnetopause and the distant tail as 5×10^{24} #/s during low solar activity, and this value is about 10% of the corresponding outflow rate of 43×10^{24} #/s. The estimated loss rate through the distant tail had been recently confirmed with STB data [*Kistler et al.*, 2010b]. However, *Ebihara et al.* [2006] argued that the percentage could vary between 37%–85%, depending on various parameters, which include geomagnetic disturbance and magnetospheric configuration. Because the CIR did not cause strong geomagnetic disturbances, we may assume the percentage is constant before and during CIR. Therefore, the total O^+ escape rate would also increase by less than 1 order. On the other hand, most of O^+ flow crossing the Martian terminator region will not return back to Mars, because the Larmor radius of an O^+ with energy of tens of eV is larger than the Mars's radius, as illustrated by *Lammer et al.* [2008, Figure 3]. Therefore, under a solar wind dynamic pressure increase by 2–3 nPa, the rate of increase in Martian O^+ escape flux could be 1 order higher than those on Earth.

[28] These observations also implicate that the distance to the Sun is crucially important because the available solar wind momentum flux is a function of the distance due to solar wind expansion. As response to the same part of the CIR body, the rate of increase in Martian O^+ outflow flux was on the same order as for Earth, though Mars has no intrinsic magnetic field. Since the mass loss rate and EUV flux from our Sun are functions of time [*Lundin et al.*, 2007], the weakly magnetized planets had little possibility to reserve their volatiles.

[29] In this work we have only discussed the influence of solar wind kinetic energy of the CIR, however, its electromagnetic energy, which can be transported into planetary magnetospheres through magnetic reconnection, is perhaps not negligible for driving ion outflow. On Earth, a CIR can usually cause continuous geomagnetic disturbance in the high-latitude ionosphere, and sometimes even affect the global ionospheric electric field [e.g., *Wei et al.*, 2008]. On Venus, *Edberg et al.* [2011] argued that the IMF polarity change across a CIR/ICME could cause dayside magnetic reconnection processes to occur in the induced magnetosphere of Venus, which would add to the erosion through associated particle acceleration. This finding may be also applied to Mars because they have similar scenario of solar wind–ionosphere interaction. As to interplanetary coronal mass ejections (ICMEs), the electromagnetic energy will play a dominant role for depositing energy to the high-latitude ionosphere at Earth [*Lu et al.*, 1998], but on Mars there is a different situation. *Pérez-de-Tejada et al.* [2009] suggested that the transport of solar wind momentum to the Mars ionosphere is more effective over the magnetic polar regions, furthermore, throughout most of the dayside hemisphere the enhanced interplanetary magnetic field (inside CME) will permeate through the upper ionosphere, and thus should make the interaction of the oncoming solar wind plasma with the ionospheric material less efficient.

[30] Both CIRs and ICMEs may play a crucial role for the evolution of planetary atmospheres. *Richardson et al.* [2002] found that the present Earth is embedded in high-speed streams ~55% for solar minimum periods, while ~35% for solar maximum. *Edberg et al.* [2011] concluded that a half (51%) of the outflow occurs during stormy space weather (CIRs and ICMEs) on Venus. Since Sun-like stars with ages of ~1 billion years are observed to have more frequent and energetic X-ray flares than those of the current Sun [*Telleschi et al.*, 2005], one could expect that stronger ICMEs were more frequently launched from the young Sun. If this is the case, as argued by *Barabash* [2010] and *Strangeway et al.* [2010], the effect of Earth's dipole collecting solar wind electromagnetic energy may be significant.

5. Summary and Conclusions

[31] We have analyzed the influence of solar wind kinetic energy of the CIR on O^+ outflow on Earth and Mars. During the CIR passage, Cluster observed an enhanced flux of upwelling oxygen ions, while MEX detected an increased escape flux of oxygen ions in the Martian magnetosphere. After comparing these observations, we found that (1) under a solar wind dynamic pressure increase of 2–3 nPa, the rate of increase in Martian O^+ outflow flux was 1 order of magnitude higher than for Earth, and (2) as a response to the same part of the CIR body, the rate of increase in Martian O^+ outflow flux was of the same order as for Earth.

[32] The results suggest that the Martian O^+ outflow is more sensitive to solar wind dynamic pressure increments than the outflow on Earth. For planetary evolution, besides having a dipolar field, the distance to the Sun is also crucially important for planetary volatile loss in our inner solar system. However, because the electromagnetic energy will become dominant during ICME passage, we still need more comparative studies (observations and simulations) of ion outflow driven by both CIR and CMEs to understand planetary atmospheric ion escape, and the role of an intrinsic magnetosphere.

[33] **Acknowledgments.** We sincerely thank the four reviewers for their valuable comments and suggestions. This work was supported by grant WO910/3-1 within the "Planetary Magnetism" priority program of the Deutsche Forschungsgemeinschaft (DFG) and through grant 50QM0801 of the German Aerospace Agency (DLR). The research conducted in China was supported by the National Science Foundation of China (grants 41004072 and 41031065) and by the National Important Basic Research Project (grant 2011CB811405). We acknowledge the CDAWeb for providing access to the STEREO merged 1-hourly in situ data, ACE, Wind, and OMNI data. The *SYMH* data are provided by the World Data Center for Geomagnetism at Kyoto University.

[34] Masaki Fujimoto thanks the reviewers for their assistance in evaluating this paper.

References

Arvelius, S., et al. (2005), Statistics of high-altitude and high-latitude O^+ ion outflows observed by Cluster/CIS, *Ann. Geophys.*, *23*, 1909–1916, doi:10.5194/angeo-23-1909-2005.

Barabash, S. (2010), Venus, Earth, Mars: Comparative ion escape rates, paper EGU2010-5308 presented at the General Assembly, Eur. Geosci. Union, Vienna, 2–7 May.

Barabash, S., et al. (2006), The analyzer of space plasma and energetic atoms (ASPERA-3) for the Mars Express mission, *Space Sci. Rev.*, *126*, 113–164, doi:10.1007/s11214-006-9124-8.

Barabash, S., A. Fedorov, R. R. Lundin, and J.-A. Sauvaud (2007), Martian atmospheric erosion rates, *Science*, *315*, 501–503, doi:10.1126/science.1134358.

Cain, J. C., B. B. Ferguson, and D. Mozzoni (2003), An $n = 90$ internal potential function of the Martian crustal magnetic field, *J. Geophys. Res.*, *108*(E2), 5008, doi:10.1029/2000JE001487.

Dennerl, K., C. M. Lisse, A. Bhardwaj, V. Burwitz, J. Englhauser, H. Gunell, M. Holmström, F. Jansen, V. Kharchenko, and P. M. Rodríguez-Pascual (2006), First observation of Mars with XMM-Newton: High resolution X-ray spectroscopy with RGS, *Astron. Astrophys.*, *451*, 709–722, doi:10.1051/0004-6361:20054253.

Dobe, Z., K. B. Quest, V. D. Shapiro, K. Szego, and J. D. Huba (1999), Interaction of the solar wind with un-magnetized planets, *Phys. Rev. Lett.*, *83*, 260–263, doi:10.1103/PhysRevLett.83.260.

Dubinin, E., M. Fränz, J. Woch, E. Roussos, S. Barabash, R. Lundin, J. D. Winningham, R. A. Frahm, and M. Acuña (2006a), Plasma morphology at Mars: Aspera-3 observations, *Space Sci. Rev.*, *126*, 209–238, doi:10.1007/s11214-006-9039-4.

Dubinin, E., et al. (2006b), Solar wind plasma protrusion into the Martian magnetosphere: ASPERA-3 observations, *Icarus*, *182*, 343–349, doi:10.1016/j.icarus.2005.08.023.

Dubinin, E., et al. (2006c), Electric fields within the Martian magnetosphere and ion extraction: ASPERA-3 observations, *Icarus*, *182*, 337–342, doi:10.1016/j.icarus.2005.05.022.

Dubinin, E., M. Fraenz, J. Woch, F. Duru, D. Gurnett, R. Modolo, S. Barabash, and R. Lundin (2009), Ionospheric storms on Mars: Impact of the corotating interaction region, *Geophys. Res. Lett.*, *36*, L01105, doi:10.1029/2008GL036559.

Dubinin, E., M. Fraenz, A. Fedorov, R. R. Lundin, N. Edberg, F. Duru, and O. Vaisberg (2011), Ion energization and escape on Mars and Venus, *Space Sci. Rev.*, *162*, 173–211, doi:10.1007/s11214-011-9831-7.

Ebihara, Y., M. Yamada, S. Watanabe, and M. Ejiri (2006), Fate of outflowing suprathermal oxygen ions that originate in the polar ionosphere, *J. Geophys. Res.*, *111*, A04219, doi:10.1029/2005JA011403.

Echer, E., et al. (2008), Cluster observations of O^+ escape in the magnetotail due to shock compression effects during the initial phase of the magnetic storm on 17 August 2001, *J. Geophys. Res.*, *113*, A05209, doi:10.1029/2007JA012624.

Edberg, N. J. T., H. Nilsson, A. O. Williams, M. Lester, S. E. Milan, S. W. H. Cowley, M. Fränz, S. Barabash, and Y. Futaana (2010), Pumping out the atmosphere of Mars through solar wind pressure pulses, *Geophys. Res. Lett.*, *37*, L03107, doi:10.1029/2009GL041814.

Edberg, N., et al. (2011), Atmospheric erosion of Venus during stormy space weather, *J. Geophys. Res.*, *116*, A09308, doi:10.1029/2011JA016749.

Engwall, E., A. I. Eriksson, C. M. Cully, M. André, R. Torbert, and H. Vaith (2009), Earth's ionospheric outflow dominated by hidden cold plasma, *Nat. Geosci.*, *2*, 24–27, doi:10.1038/ngeo387.

Frahm, R. A., et al. (2006), Carbon dioxide photoelectron energy peaks at Mars, *Icarus*, *182*, 371–382, doi:10.1016/j.icarus.2006.01.014.

Fränz, M., et al. (2006), Plasma intrusion above Mars crustal fields—Mars Express ASPERA-3 observations, *Icarus*, *182*, 406–412, doi:10.1016/j.icarus.2005.11.016.

Fränz, M., E. Dubinin, E. Nielsen, J. Woch, S. Barabash, R. Lundin, and A. Fedorov (2010), Transterminator ion flow in the Martian ionosphere, *Planet. Space Sci.*, *58*, 1442–1454, doi:10.1016/j.pss.2010.06.009.

Kistler, L. M., C. G. Mouikis, B. Klecker, and I. Dandouras (2010a), Cusp as a source for oxygen in the plasma sheet during geomagnetic storms, *J. Geophys. Res.*, *115*, A03209, doi:10.1029/2009JA014838.

Kistler, L. M., et al. (2010b), Escape of O^+ through the distant tail plasma sheet, *Geophys. Res. Lett.*, *37*, L21101, doi:10.1029/2010GL045075.

Lammer, H., J. F. Kasting, E. Chassefière, R. E. Johnson, Y. N. Kulikov, and F. Tian (2008), Atmospheric escape and evolution of terrestrial planets and satellites, *Space Sci. Rev.*, *139*, 399–436, doi:10.1007/s11214-008-9413-5.

Lu, G., et al. (1998), Global energy deposition during the January 1997 magnetic cloud event, *J. Geophys. Res.*, *103*(A6), 11,685–11,694, doi:10.1029/98JA00897.

Luhmann, J. G., W. T. Kasprzak, and C. T. Russell (2007), Space weather at Venus and its potential consequences for atmosphere evolution, *J. Geophys. Res.*, *112*, E04S10, doi:10.1029/2006JE002820.

Lundin, R., et al. (2004), Solar wind-induced atmospheric erosion at Mars: First results from ASPERA-3 on Mars Express, *Science*, *305*, 1933–1936, doi:10.1126/science.1101860.

Lundin, R., H. Lammer, and I. Ribas (2007), Planetary magnetic fields and solar forcing: Implications for atmospheric evolution, *Space Sci. Rev.*, *129*, 245–278, doi:10.1007/s11214-007-9176-4.

Lundin, R., S. Barabash, M. Holmström, H. Nilsson, M. Yamauchi, M. Fraenz, and E. M. Dubini (2008a), A comet-like escape of ionospheric plasma from Mars, *Geophys. Res. Lett.*, *35*, L18203, doi:10.1029/2008GL034811.

Lundin, R., S. Barabash, A. Fedorov, M. Holmström, H. Nilsson, J.-A. Sauvaud, and M. Yamauchi (2008b), Solar forcing and planetary ion escape from Mars, *Geophys. Res. Lett.*, *35*, L09203, doi:10.1029/2007GL032884.

McEnulty, T. R., J. G. Luhmann, I. de Pater, D. A. Brain, A. Fedorov, T. L. Zhang, and E. Dubinin (2010), Interplanetary coronal mass ejection influence on high energy pick-up ions at Venus, *Planet. Space Sci.*, *58*, 1784–1791, doi:10.1016/j.pss.2010.07.019.

Moore, T. E., and J. L. Horwitz (2007), Stellar ablation of planetary atmospheres, *Rev. Geophys.*, *45*, RG3002, doi:10.1029/2005RG000194.

Moore, T. E., W. K. Peterson, C. T. Russell, M. O. Chandler, M. R. Collier, H. L. Collin, P. D. Craven, R. Fitzenreiter, B. L. Giles, and C. J. Pollock (1999), Ionospheric mass ejection in response to a CME, *Geophys. Res. Lett.*, *26*(15), 2339–2342, doi:10.1029/1999GL900456.

Nilsson, H., et al. (2004), The structure of high altitude O^+ energization and outflow: A case study, *Ann. Geophys.*, *22*, 2497–2506, doi:10.5194/angeo-22-2497-2004.

Pérez-de-Tejada, H. (1998), Momentum transport in the solar wind erosion of the Mars ionosphere, *J. Geophys. Res.*, *103*(E13), 31,499–31,508, doi:10.1029/1998JE900001.

Pérez-de-Tejada, H., R. Lundin, H. Durand-Manterola, and M. Reyes-Ruiz (2009), Solar wind erosion of the polar regions of the Mars ionosphere, *J. Geophys. Res.*, *114*, A02106, doi:10.1029/2008JA013295.

Pérez-de-Tejada, H., M. Reyes-Ruizb, and H. Durand-Manterola (2010), Viscous flow properties in the transport of solar wind momentum to the Venus upper ionosphere, *Icarus*, *206*, 182–188, doi:10.1016/j.icarus.2009.05.023.

Pollock, C. J., M. O. Chandler, T. E. Moore, J. H. Waite Jr., C. R. Chappell, and D. A. Gurnett (1990), A survey of upwelling ion event characteristics, *J. Geophys. Res.*, *95*(A11), 18,969–18,980, doi:10.1029/JA095iA11p18969.

Rème, H., et al. (2001), First multispacecraft ion measurements in and near the Earth's magnetosphere with the Identical Cluster Ion Spectrometry (CIS) experiment, *Ann. Geophys.*, *19*, 1303–1354, doi:10.5194/angeo-19-1303-2001.

Richardson, I. G., H. V. Cane, and E. W. Cliver (2002), Sources of geomagnetic activity during nearly three solar cycles (1972–2000), *J. Geophys. Res.*, *107*(A8), 1187, doi:10.1029/2001JA000504.

Seki, K., R. C. Elphic, M. Hirahara, T. Terasawa, and T. Mukai (2001), On atmospheric loss of oxygen ions from Earth through magnetospheric processes, *Science*, *291*, 1939–1941, doi:10.1126/science.1058913.

Strangeway, R. J., C. T. Russell, J. G. Luhmann, T. E. Moore, J. C. Foster, S. V. Barabash, and H. Nilsson (2010), Does a planetary-scale magnetic field enhance or inhibit ionospheric plasma outflows? Abstract SM33B-1893 presented at 2010 Fall Meeting, AGU, San Francisco, Calif., 13–17 Dec.

Telleschi, A., et al. (2005), Coronal evolution of the Sun in time: High-resolution X-ray spectroscopy of solar analogs with different ages, *Astrophys. J.*, *622*, 653–679, doi:10.1086/428109.

Tsyganenko, N. A. (1995), Modeling the Earth's magnetospheric magnetic field confined within a realistic magnetopause, *J. Geophys. Res.*, *100*(A4), 5599–5612, doi:10.1029/94JA03193.

Vignes, D., C. Mazelle, H. Rme, M. H. Acuña, J. E. P. Connerney, R. P. Lin, D. L. Mitchell, P. Cloutier, D. H. Crider, and N. F. Ness (2000), The solar wind interaction with Mars: Locations and shapes of the bow shock and the magnetic pile-up boundary from the observations of the MAG/ER Experiment onboard Mars Global Surveyor, *Geophys. Res. Lett.*, *27*(1), 49–52, doi:10.1029/1999GL010703.

Wei, Y., M. Hong, W. Wan, A. Du, J. Lei, B. Zhao, W. Wang, Z. Ren, and X. Yue (2008), Unusually long lasting multiple penetration of interplanetary electric field to equatorial ionosphere under oscillating IMF Bz, *Geophys. Res. Lett.*, *35*, L02102, doi:10.1029/2007GL032305.

Yau, A. W., and M. Andre (1997), Sources of ion outflow in the high latitude ionosphere, *Space Sci. Rev.*, *80*, 1–25, doi:10.1023/A:1004947203046.

Yau, A. W., W. K. Peterson, and E. G. Shelley (1988), Quantitative parametrization of energetic ionospheric ion outflow, in *Modeling Magnetospheric Plasma*, *Geophys. Monogr. Ser.*, vol. 44, edited by T. E. Moore et al., pp. 211–217, AGU, Washington, D. C., doi:10.1029/GM044p0211.

Zhang, J.-C., L. M. Kistler, C. G. Mouikis, H. Matsui, B. Klecker, I. Dandouras, and M. W. Dunlop (2011), Shock-driven variation in ionospheric outflow during the 11 October 2001 moderate storm, *J. Geophys. Res.*, *116*, A00J18, doi:10.1029/2010JA015627.

S. Barabash and R. Lundin, Swedish Institute of Space Physics, Box 812, SE-981 28 Kiruna, Sweden.

I. Dandouras, Research Institute in Astrophysics and Planetology, National Center for Scientific Research, PO Box 44346, 9 Ave. du Colonel Roche, F-31028 Toulouse, France.

E. Dubinin, M. Fraenz, Y. Wei, and J. Woch, Max Planck Institute for Solar System Research, Max-Planck Str. 2, D-37191 Katlenburg-Lindau, Germany. (fraenz@mps.mpg.de; wei@mps.mpg.de)

S. Y. Fu, Z. Y. Pu, and Q.-G. Zong, School of Earth and Space Sciences, Peking University, 100871 Beijing, China.

H. Lühr, German Research Centre for Geosciences, Telegrafenberg, F 456 D-14473 Potsdam, Germany.

W. Wan, Institute of Geology and Geophysics, Chinese Academy of Sciences, 19 Beitucheng Western Rd., Chaoyang District, 100029 Beijing, China.

T. L. Zhang, Space Research Institute, Austrian Academy of Sciences, Schmiedlstraße 6, 8042 Graz, Austria.